# Boundary Detection of Altered Region by Differential Features on Camera Response Function

Hirokazu Kato
Criminal Investigation Laboratory, Tottori Prefectural Police Headquarters 2-12, chiyomi, Tottori-shi, Tottori, 680-0911 Japan

Toshiyuki Nagao, Hideaki Fujiwara, and Katsuya Kondo
Dept. Information and Electronics, Graduate School of Eng. Tottori University 4-101, Koyama-cho Minami, Tottori-shi, Tottori, 680-8552 Japan
E-mail: {b07t3039, b08t3057}@faraday.ele.tottori-u.ac.jp, kondo@ele.tottori-u.ac.jp

***Abstract*—An image splicing can be easily made by a skilled image editor, and verification of authentic image has become important. In this paper, we propose a detection method for splicing boundaries that uses uniformity on camera response function (CRF) in an image. This uniformity is observed as differential features of CRF. In altered image, the non-uniformity of CRF mostly appears on the edges of a splicing region. The characteristics of CRF extracted from edges in an image differ between an altered region and an authentic region. We analyze these characteristics by using QR map. The QR map represents the relation between this features and image intensity. An authentic boundary has the characteristics of a common CRF within an image, but a splicing boundary is not so. We show the tendency of authentic boundaries in QR map, and we argue about the method of estimating whether a target boundary is spliced by evaluating the consistency of QR map.**

***Index Terms*—camera response function, splicing boundary, QR map, digital forensics**

## I. Introduction

An image can be edited by using the high functionality of image editing software. Given this situation, there is sometimes editing and splicing of images to create images unintended by the photographer, and being unsure of whether the digital image is real or not makes it difficult to certify it as authentic. In response, digital watermarking is used as means of verifying an image's authenticity. This is a method of detecting alteration by embedding information within the image; however, it requires embedding of the information in advance. Therefore, a detection method of altered region which do not need embedded information has become important.

In this paper, we estimate the camera response function (CRF) as shown in Fig. 1 and investigate the consistency of the response function within the image in order to detect whether the image has been spliced. That is, the CRF has a consistency within an original image; however, within an altered image, some different CRFs are included, as shown in Fig. 2. The characteristics can be used for detecting altered regions. The CRF is not generally known. In order to analyze and estimate CRF, many methods have been proposed [1]-[4]. K. Ikeuchi *et al.* used several images of the same static scene taken from the same view point to estimate it accurately in the presence of noise [1]. S. Lin *et al*. have achieved radiometric calibration from an image, based on RGB distributions at edges [3]. Also, S. F. Chang *et al*. have defined the geometrical invariant (GI) as CRF differentiation, which is a camera-specific invariant obtained from the gradient information around the edges [5]-[8]. The method can estimate it from a piece of image. We focus on splicing boundaries between altered area and authentic area. And we analyze the features of splicing boundaries differing from those of a normal edge area and discuss a method for detecting altered regions from a single image.

In this paper, we detect the existence of an alteration by investigating this tendency. The paper is organized as follows: In Section II, we clarify the principles of alteration detection, Section III describes a method for comparing an authentic boundary and a splicing boundary by using the differential features, and Section IV describes a method for detecting splicing boundaries. In Section V, some experimental results are shown. Finally, Section VI concludes the paper.

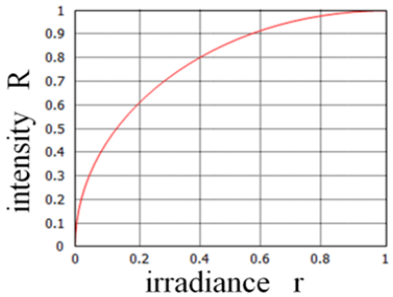


Figure 1. Camera response function

Manuscript received January 30, 2014; revised April 24, 2014.


doi: 10.12720/ijsps.2.1.31-36

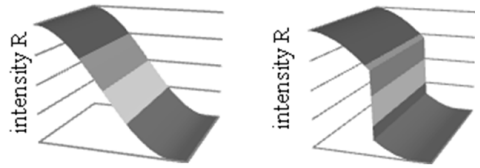


(a) Authentic boundary (b) Splicing boundary

Figure 2. Intensity distribution on boundaries

## II. ESTIMATING CRF

Y. F. Hsu *et al*. focused on whether there was consistency within an image using CRF for alteration detection [8]. As shown in Fig. 3, the image suspected to be spliced is divided into three regions of the region 1 taken by camera 1, the region 2 by camera 2, and the region 3 on the boundary of these first two regions. This boundary region 3 is an area where a spliced edge potentially exists. Each CRF is respectively estimated in regions 1 and region 2 by the method of *Tian T. Ng*. In the case of altered image, there is a significant difference in CRFs between region 1 and region 2. This difference is used to evaluate whether an image has been spliced. However this approach has a problem when textures have low intensity around target boundaries. That is, for the image which has a smaller difference in CRFs, it is difficult to detect altered regions. And so, we investigate a method of detecting the alteration in the case that some textures in an image partly have low intensity.

For alteration detection, we use the *Tian*'s method using geometrical invariant (GI) as CRF differentiation. First, the candidates of splicing boundaries are analyzed by this GI. For the analysis, we use a QR map which expresses the relationship between GI and image intensity, and shows the significant difference between authentic boundaries and splicing boundaries.

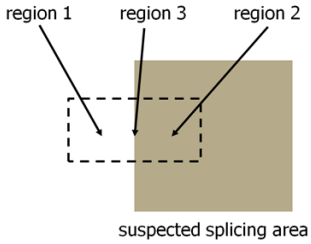


Figure 3. Division of the splicing region

### A. Definition of Camera Response Function (CRF)

CRF is a function for converting the irradiance, as light energy incident on the image sensor, into image intensity. So, CRF is generally expressed as $R=f(r)$, where $R$ is the image intensity and $r$ is the light energy incident on the image sensor. CRF is generally unknown because it varies by device and photography setting, and it is known to be a non-linear function as shown in Fig. 1. CRF is modeled as a gamma curve, $f(r)=r^{\gamma}$. However, because the actual CRF cannot be expressed by this gamma curve model in a precise sense, this function can be expressed by a polynomial expression as equation (1). And we show two expression of CRF as follow, $f: r \to R, g: R \to r$.

$$f(r)=r^{P(r,\tilde{\alpha})} \text{ and } g(R)=R^{1/P(R,\tilde{\alpha})} \tag{1}$$

where $\tilde{\alpha}=[\alpha_0,\ldots,\alpha_n], P(r,\tilde{\alpha})=\sum_{i=0}^{n}\alpha_i r^i$. Furthermore, $\tilde{\alpha}$ is the $\gamma$ parameter, and equation (1) can be expressed as $f(r)=r^{\alpha_0+\alpha_1 r}$.

### B. Geometrical Invariance (GI)

The CRF in the coordinates of image is expressed as $R(x, y) = f(r(x, y))$. Then, GI is defined as equation (2).

$$\frac{R_{xx}}{R_x^2}=\frac{R_{yy}}{R_y^2}=\frac{R_{xy}}{R_x R_y}=\frac{f''\left(f^{-1}(R)\right)}{\left(f'\left(f^{-1}(R)\right)\right)^2}=GI(R) \tag{2}$$

where $R_x$, $R_y$ are the first-order derivatives in the $x$-direction and $y$-direction, respectively. And $R_{xx}$, $R_{yy}$, $R_{xy}$ are the corresponding second-order derivatives. As expressed in equation (2), GI can be defined in terms of the derivatives of CRF, but also in terms of the derivatives of $R$. Moreover the GI can be determined from the majority of edges in an image. It can be obtained from the intensity in an image without irradiance. Therefore it is possible to estimate CRF by analyzing GI. CRF is modeled as equation (1), but it can be simply expressed as $f(r)=r^{\gamma}$. Thus, the relationship between the gamma curve model and GI, is expressed as

$$\gamma=\frac{1}{1-GI(R)R}=Q(R). \tag{3}$$

### C. Estimation of Parameter γ

The CRF estimation means estimating the parameter $\gamma$ in the gamma curve model. And the parameter $\gamma$ of equation (3) is extended to a polynomial function in equation (4).

$$Q(R)=\frac{(\alpha_1 r\, ln(r)+\alpha_1 r+\alpha_0)^2}{\alpha_0-\alpha_1 r} \tag{4}$$

In equation (4), $Q(R)$ can be obtained by equation (3), and the parameter $r$ can be obtained by $R$ in equation (1). However, as it is not possible to obtain the parameters $\alpha_0$, $\alpha_1$ directly, instead they can be estimated as

$$\tilde{\alpha}^*=\arg\min_{(\alpha_0,\alpha_1)}\sum_{j,k}P(Q_j \mid R_k)|Q_j-Q(R_k,\tilde{\alpha})|^2 \tag{5}$$

where $\tilde{\alpha}=(\alpha_0,\alpha_1)$, and $\tilde{\alpha}^*$ is an estimated parameter. Furthermore, $Q_j$ is the value of GI obtained from an image. $P(Q_j \mid R_k)$ means to be a weight factor. The GI includes some factors unsuitable for estimating of CRF, and the weight term is used to minimize the effect (see reference [6] for a detailed definition).

## III. CHARACTERISTICS OF SPLICING BOUNDARY

The characteristics of GI change in dependence on the shapes of boundaries. Here we explain the differences between the behavior of a splicing boundary and that of an authentic boundary. The differences of characteristics

between the authentic and splicing boundaries are shown in Fig. 2. While the authentic boundary shows consecutive and smooth changes in intensity, splicing boundary in an altered image presents drastic and sharp changes in intensity. Furthermore, in Fig. 3, the areas suspected of being spliced are divided into three regions. As region 1 and region 2 are images captured by different cameras, their CRF differs from each other. And region 3, which is the boundary, is considered to have a CRF that is not natural characteristics in the case of altered image. Therefore, GI of the splicing region 3 has a behavior different from an authentic image.

### A. QR Map

The QR map is $Q(R)$ in equation (3), plotted as a scatter diagram. An example is shown in Fig. 4. The horizontal axis expresses the intensity $R$ and the vertical axis expresses $Q(R)$. White points in Fig. 4 express GI, and the solid line presents a curve of a parameter $\gamma$ estimated from equation (5). $Q(R)$ basically has an approximately uniform distribution for a given intensity.

CRF is consistent within an image. However, as the estimates of $Q(R)$ is limited when estimating from only one part of the image, the distribution of $Q(R)$ often deviates from original characteristics and it is often not to be a unique CRF. Therefore, a simple comparison of the estimated CRF in each region is not a particularly good method for judging whether a region includes a splice.

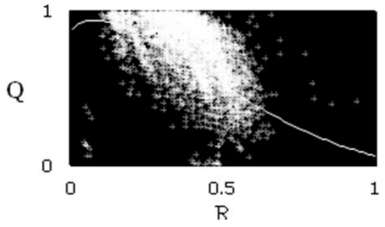


Figure 4. QR map

### B. Difference between Splicing and Authentic Boundary

We explain about the differences between a splicing boundary and authentic boundary in terms of the QR map. Fig. 5(a) and Fig. 5(b) express QR maps of the splicing and authentic boundaries. $R$ is normalized from 0 to 1.

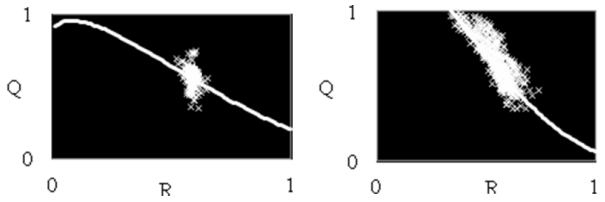


(a) Splicing boundary (b) Authentic boundary

Figure 5. Comparison of QR map

The QR map for an authentic boundary, when it is compared with that of the splicing boundary, has a distribution in a form that matched the estimated curve of CRF. The distribution of authentic is uniform within the profile. In contrast, the splicing boundary is often concentrated around a local area, as shown in Fig. 5(a). The distribution profiles present different tendencies for the splicing and authentic boundaries. However, there is no clear difference at the Root Mean Square Error (RMSE) of these estimated curves, $Q(R)$, in order to distinguish between authentic and splicing boundaries.

Although there are differences in the distribution profile, $Q(R)$ of authentic boundary is distributed adjacent to the estimated curve. The RMSE between the estimated curve and $Q(R)$ has a tendency to be affected more by the texture of background than whether it is an authentic or splicing boundary. In the region where there has high intensity of texture in the boundary, the distribution in the QR map spreads regardless of whether it is authentic or spliced. Therefore, it is difficult to distinguish it based solely on the RMSE between the distribution and estimated curve. However, it can be distinguished by finding the similarity of the estimated curve and $Q(R)$ distribution profiles.

## IV. Comparison of Estimated Curve and Distribution Profile

In Section III-B, we stated that the QR map of an authentic boundary has a tendency to better match the CRF estimated curve. In other words, the shape of the distribution profile for authentic boundary in the QR map is similar to that of the estimated curve. For this reason, we can artificially estimate a distribution profile that follows the shape of the estimated curve. The detection of altered region can be performed by comparing the estimated distribution in the QR map with actual distribution. And when actual distribution resembles an estimated distribution, that is, it resembles a distribution of authentic boundary, we assume it an authentic boundary, but when it do not resemble, we assume it a splicing boundary.

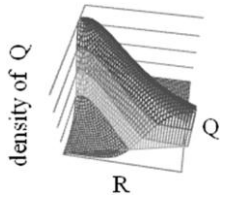


Figure 6. Density distribution of Q in QR map

Fig. 6 shows the estimated distribution based on the curve. The horizontal and depth axes express intensity and $Q(R)$, and the vertical axis indicates the density of $Q$. The density of $Q$ has a high value, when $Q(R)$ is distributed with high probability. Therefore, the estimated distribution profile is set the highest value on the CRF estimation curve and a lower value further away from the curve. We let the profile of the density of $Q$ be a normal distribution. The correlation shown in equation (6) is investigated as a method for comparing the assumed distribution and actual observed distribution.

$$R_N = \frac{\sum\sum f(x,y)g(x,y)}{\sqrt{\sum\sum f(x,y)^2}\sqrt{\sum\sum g(x,y)^2}} \qquad (6)$$

where $x$, $y$ are the QR map coordinates, $f(x, y)$ is the $Q(R)$ distribution estimated from the CRF estimated curve, and

$g(x, y)$ is the $Q(R)$ distribution actually observed. The correlation of an authentic boundary should be high, whereas that for splicing boundary should be relative low, because a splicing boundary tends to be concentrated around a local area. These differences can be used to judge whether a boundary is a splicing boundary.

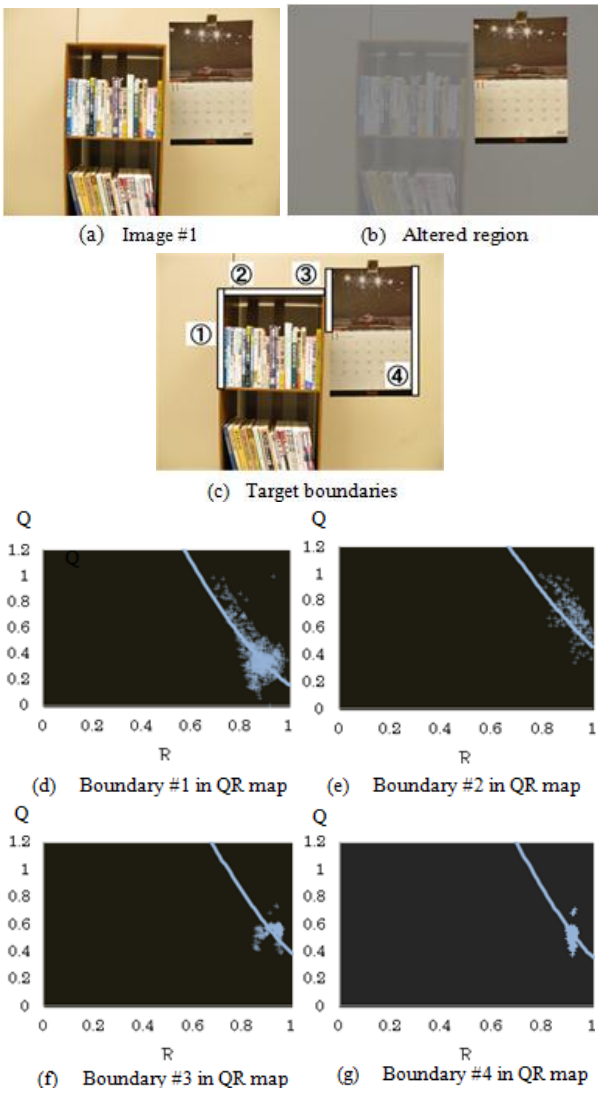


Figure 7. QR maps of image #1

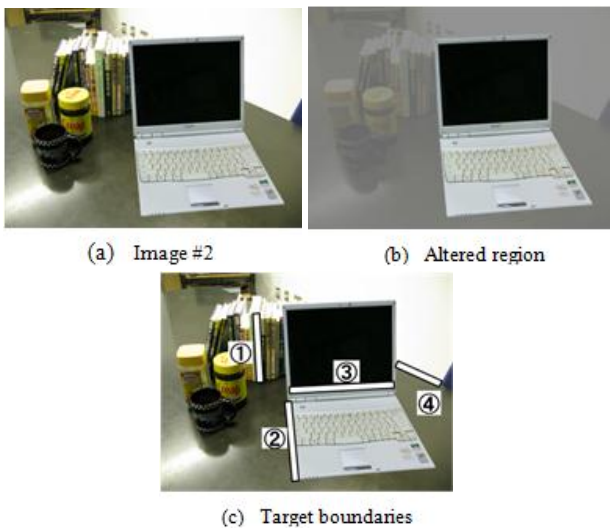


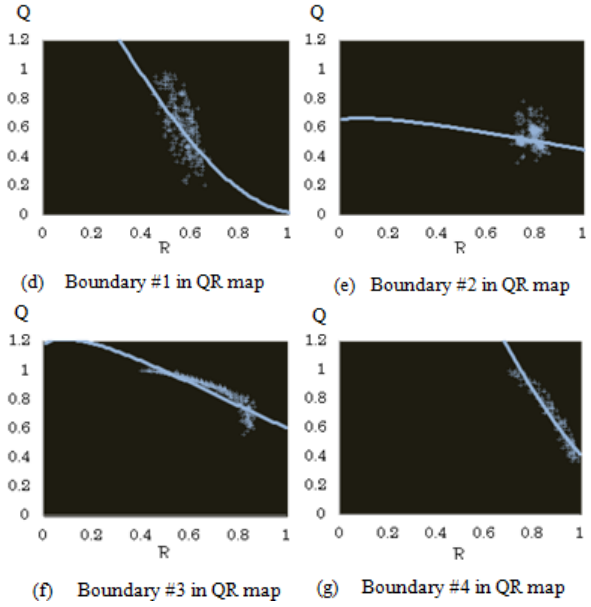


Figure 8. QR maps of image #2

TABLE I. CORRELATION VALUES

| | Boundary #1 | Boundary #2 | Boundary #3 | Boundary #4 |
|---|---|---|---|---|
| Image #1 | 0.3888 | 0.3947 | 0.1666 | 0.1508 |
| Image #2 | 0.3443 | 0.1534 | 0.2849 | 0.3854 |

## V. EXPERIMENT AND DISCUSSION

For the present study, we took multiple boundaries from an image that included a splicing boundary and investigated whether it can be identified as a spliced image. This was done by taking the correlation between the respective QR map profile and the QR map estimated from the CRF estimated curve.

We investigated using the method discussed in Section IV. Specifically, we evaluated multiple boundaries extracted from a single image and analyzed whether each was a splicing boundary. For the experiment, the variance in the normal distribution was set as 0.25. The boundary was divided into RGB regions, and the correlation values are respectively taken the average. Fig. 7(a) and Fig. 8(a) show the altered images for experiments. The spliced regions in these images were the calendar and computer, as shown in Fig. 7(b) and Fig. 8(b). Fig. 7(c) and Fig. 8(c) express the boundaries extracted from the respective images. The results of calculating the correlation of the QR distribution profile and the QR distribution assumed from the CRF estimated curve are shown in Table I.

For experimental image #1, the total boundaries were divided into two groups: boundaries #1 and #2, and boundaries #3 and #4. The correlation values for the first group are high, compared with those for the latter group, which is characteristic of splicing boundaries. The total boundaries can be distinguished as a splicing boundary from Fig. 7(b) and Fig. 7(c). Boundaries in experimental image #2 reveals the same results as those revealed for experimental image #1, that is, the boundaries of #1, #3 and #4 show the characteristics of being an authentic boundary, and the boundary #2 can be distinguished as

the splicing one. Experimental image #3 compares the correlation values of authentic and splicing boundaries. The authentic boundaries #1-4 have a higher correlation than the splicing boundaries #5-8 as shown in Fig. 9(d). For experimental images #4 and #5, the QR maps of the extracted boundaries in the RGB plane are shown in Fig. 10 and Fig. 11. The distribution profiles were discontinuous because there are few GI. The reason is that a tendency of the density resembles splicing. Although the distribution in the QR map differs by each RGB plane of image #4 as shown in Fig. 10(f), and image #5 in Fig. 11(e), the distribution profiles resemble the other distribution profiles in each plane. That is, the correlation values for the boundaries #1-2 of image #4-5 are low, compared with those for #3-4 from Table II.

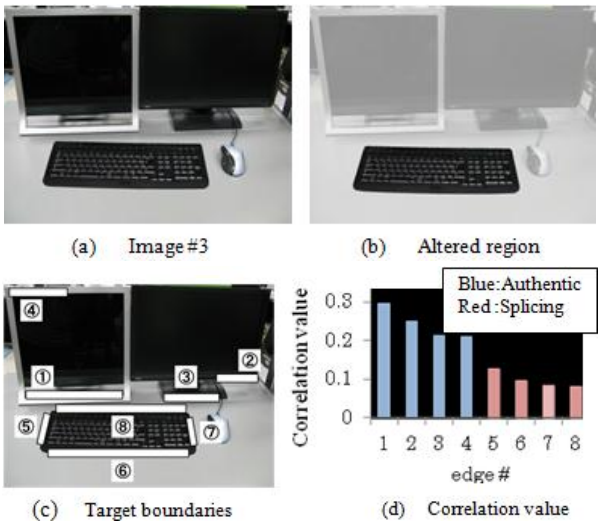


Figure 9. QR maps of image #3

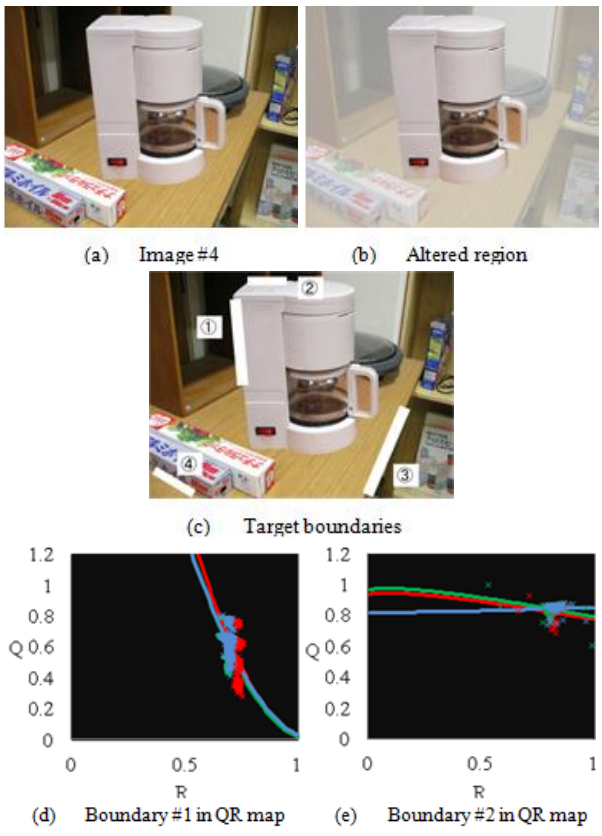


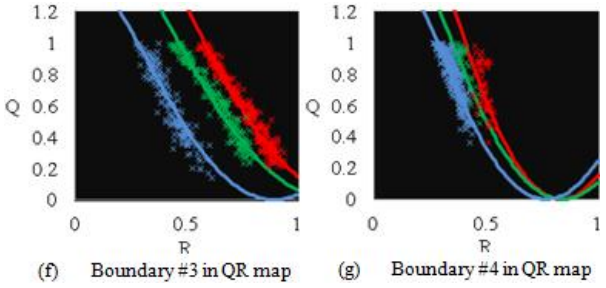


Figure 10. QR maps of image #4

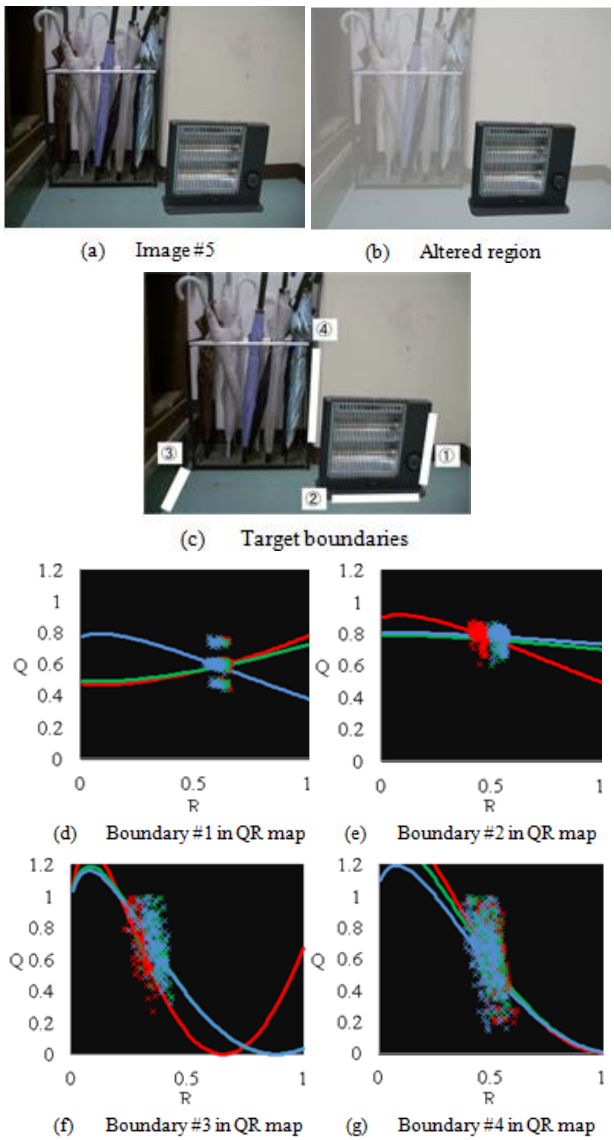


Figure 11. QR maps of image #5

TABLE II. CORRELATION VALUES

| | | Boundary #1 | Boundary #2 | Boundary #3 | Boundary #4 |
|---|---|---|---|---|---|
| Image #4 | R | 0.1392 | 0.1026 | 0.4541 | 0.2212 |
| | G | 0.1523 | 0.1007 | 0.3816 | 0.2010 |
| | B | 0.1579 | 0.0778 | 0.3481 | 0.3149 |
| Image #5 | R | 0.0964 | 0.1045 | 0.2475 | 0.3539 |
| | G | 0.0769 | 0.0902 | 0.2828 | 0.3336 |
| | B | 0.1063 | 0.1014 | 0.3022 | 0.3385 |

## VI. Conclusion

In order to verify authentic images such as evidence photographs, we performed splicing boundary detection by analyzing GI while estimating CRF. We used the characteristic that CRF have consistency within an original image. For an authentic image, the distribution in the QR map always follows the shape of the CRF estimated curve, whereas for a splicing boundary, the distribution would be concentrated in a local area. We focused on the differences between the profiles of distribution in the QR map. And by taking a correlation between the actual distribution profile and the distribution assumed from the CRF estimated curve in the QR map, it is possible to distinguish between a splicing boundary and an authentic boundary. In future work, we will investigate boundaries where smoothing is performed on altered region and the changes in intensity on boundaries are smooth.

## References


[1] J. Takamatsu, Y. Matsushita, and K. Ikeuchi, "Estimating camera response functions using probabilistic intensity similarity," in *Proc. IEEE Int'l Conf. Computer Vision and Pattern Recognition*, Jun. 2008, pp.1-8.

[2] D. Grossberg and S. K. Nayar, "What is the space of camera response functions," in *Proc. IEEE Int'l Conf. Computer Vision and Pattern Recognition*, Jun. 2003, pp. 602-609.

[3] S. Lin, G. Jinwei, S. Yamazaki, and S. Y. Heung: "Radiometric calibration from a single image," in *Proc. IEEE Int'l Conf. Computer Vision and Pattern Recognition*, Jun./Jul. 2004, pp. 938-945.

[4] T. T. Ng, "Statistical and geometric methods for passive-blind image forensics," PhD Thesis, Graduate School of Arts and Sciences, Columbia Univ., May 2007.

[5] Y. F. Hsu and S. F. Chang, "Camera response functions for image forensics: An automatic algorithm for splicing detection," *IEEE Trans. on Information Forensics and Security*, vol. 5, no. 4, pp. 816-825, Dec. 2010.

[6] T. T. Ng, S. F. Chang, M. P. Tsui, "Using geometry invariants for camera response function estimation," in *Proc. IEEE Int'l Conf. Computer Vision and Pattern Recognition*, Jun. 2007, pp. 1-8.

[7] T. T. Ng and S. F. Chang, "Camera response function estimation from a single-channel image using differential invariants," ADVENT Technical Report #216-2006-2, Mar. 2006.

[8] Y. F. Hsu and S. F. Chang, "Detecting image splicing using geometry invariants and camera characteristics consistency," in *Proc. Int'l Conf. on Multimedia and Expo*, Jul. 2006, pp.549-552.


**Hirokazu Kato** received his B.E. degree in electronic engineering from University of Electro-Communications, Japan in 1998. He is now with the Criminal Investigation Laboratory, Tottori Prefectural Police Headquarters. His current research interests include Judgment and research adapting physics.

**Toshiyuki Nagao** received his B.E., M.E. degrees in electrical and electronic engineering from Tottori University, Tottori, Japan in 2011, 2014, respectively. His current research interests include digital forensics technology.

**Hideaki Fujiwara** received his B.E., M.E. degrees in electrical and electronic engineering from Tottori University, Tottori, Japan in 2012, 2014, respectively. His current research interests include image processing.

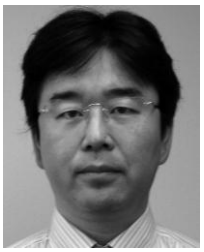

**Katsuya Kondo** is a Professor at the Department of Information and Electronics, Graduate School of Engineering, Tottori University, Tottori, Japan. He received the B.E., M.E., and D.E. degrees in electrical engineering from Keio University, Yokohama, Japan, in 1989, 1991, and 1997, respectively. From 2002 to 2008, he was an Associate Professor at the Division of Computer Engineering, Graduate School of Engineering, University of Hyogo, Hyogo, Japan. His current research interests are in the application and theory of multidimensional signal processing. He is a member of the Institute of Electronics, Information and Communication Engineers, the Institute of Image Information and Television Engineers, the Society of Instrument and Control Engineers, and IEEE.

 